

Predictive Direct Power Control and Fuzzy Logic Control of the Three Phase Grid-connected Converter

^[1]R.P.Anitha, ^[2]M.Inba Arasi

^[1] PG Student, Mahendra College of Engineering, Minnampalli, Salem,

^[2] Assistant Professor, Mahendra College of Engineering, Minnampalli, Salem.

^[1]rp.anitha981@gmail.com, ^[2]inbaarasivijayan@gmail.com

Abstract: In this paper, a predictive direct power control (DPC) method without sector information and voltage vector selection is proposed for three-phase grid-connected converters. Different from conventional predictive direct power controllers, the proposed strategy always adopts fixed voltage vectors, instead of selecting voltage vectors according to the angular information of the grid-voltage vector or the virtual-flux vector. The converter switching time is obtained by minimizing the squared errors of the instantaneous active and reactive power. Switch duty cycles are then calculated and equivalently reconstructed. The proposed strategy not only presents rapid dynamic response due to the use of the predictive controller, but also possesses excellent steady state performance as a result of duty cycle reconstruction. The main advantage of the proposed control scheme, compared with the classical DPC strategies, is that it is unnecessary to use sector information of the grid-voltage vector, and selection of active voltage vectors is also not required here. Therefore, incorrect selection of voltage vectors and the resulting performance deterioration are surely avoided, without the need of any additional compensation measures. An in-depth comparison and experimental assessment are given to validate the effectiveness of the proposed strategy.

Index Terms— Cost function minimization, Duty cycle reconstruction, Predictive direct power control (P-DPC), Voltage vector selection.

I. INTRODUCTION

In a broad variety of application areas, such as electrical drives and distributed power generations, three-phase converters are often adopted to connect the electrical system to the unity grid. Their control strategies have garnered increasing attention over the last decades [1], [2]. Nowadays, different kinds of control strategies have been presented in technical literature. Direct power control (DPC) emerges as a new alternative for voltage-oriented vector control [3]–[6]. It adopts power controllers instead of current control loops. During its implementation process, a lookup table [7]–[9] or predefined selecting rules [10] are previously constructed based on instantaneous power behaviors of the converter. The optimal switching state is selected according to the errors between the measured and the reference values of active and reactive powers, as well as the information of

the grid voltage vector [11] or the estimated virtual flux vector [12]. However, the resulting variable switching frequency leads to several problems. A relatively high sampling frequency is usually required in order to obtain acceptable control performances [13]. Furthermore, in order to enhance the robustness of DPC and overcome problems associated with system parameter uncertainties, adaptive techniques have been included in the design of DPC laws,

and therefore, the performance of the whole system is thus less sensitive to system parameters values uncertainties and variations [14], [15].

Another approach for implementing DPC for three-phase grid-connected converters is to take advantage of model predictive control strategies [16]–[18], in which the discrete nature of converters is taken into account in order to predict the future behaviors of the system [19]–[21]. The converter behaviors are predicted only for the possible switching states, and the optimal state with minimum cost is then selected and applied. This method presents fast dynamic responses as well as generating sinusoidal currents without any modulators. However, the current spectrum is distributed over a range of frequencies, which complicates the design of the grid filter. Therefore, the authors of [22] present a predictive DPC technique using dead beat control principle. Besides, predictive DPC (P-DPC) algorithms based on predictive selection of voltage-vectors' sequences are proposed in [23] and [24]. Within each sampling period, this method first selects two active voltage vectors according to the angular information of the grid-voltage vector [25] or the space vector position of the virtual flux [26]. The action time sequence is then calculated by minimizing the cost function, which is constructed based on the errors between the predicted and the reference values of active and reactive powers. The calculated optimal time

sequence is then transferred to the modulation block, and consequently, the switch signals are obtained. By combining predictive approach with DPC theory, this algorithm provides both high transient dynamics and constant switching frequency.

II. IMPLEMENTATION OF PDPC

Obviously, when P-DPC is implemented, selection of active voltage vectors is essential and plays an important role, which is based on the knowledge of the position of the grid-voltage vector.

TABLE I Selected Voltage Vectors Within Different Sectors

Sector Number	Selected voltage vectors
I	$\{V_0, V_1, V_2, V_7\}$ or $\{V_0, V_1, V_6, V_7\}$
II	$\{V_0, V_2, V_3, V_7\}$ or $\{V_0, V_1, V_2, V_7\}$
III	$\{V_0, V_3, V_4, V_7\}$ or $\{V_0, V_2, V_3, V_7\}$
IV	$\{V_0, V_4, V_5, V_7\}$ or $\{V_0, V_3, V_4, V_7\}$
V	$\{V_0, V_5, V_6, V_7\}$ or $\{V_0, V_4, V_5, V_7\}$
VI	$\{V_0, V_6, V_1, V_7\}$ or $\{V_0, V_5, V_6, V_7\}$

Besides, it is found that the selection method widely used in conventional P-DPC might result in incorrect selection of voltage vectors. Therefore, the calculated value of the voltage vector action time may be negative. Conventionally, the action time is normally forced to zero whenever a negative value is predicted, resulting in control failures and performance deterioration. In order to solve this problem, references [27], [28] and [29] proposed effective solutions. In [30], a generalized PDPC strategy for ac/dc converters is proposed. Based on the analysis of power characteristics, a novel method of optimal voltage vector selection is developed. A least-square cost function is evaluated with respect to different sectors. Global optimal voltage vectors are thus selected by means of cost function minimization. In [31] and [32], compensation measures are added to conventional P DPC. Whenever negative time values come out, the active voltage vectors are reselected based on the modified lookup table. In other words, active voltage vectors should be selected twice when the calculated value of the voltage-vector action time is smaller than zero. The objective of this paper is to propose an improved predictive DPC method without sector information of the grid voltage and without voltage vector selection process. Obviously, the proposed strategy simplifies the DPC method. Furthermore, the appearance of negative time values is completely avoided, and there is no need to take any additional compensation measures. The rest of this paper is organized as follows. Section III describes the operation principle of conventional predictive DPC strategies based on voltage vector selection. Detailed analysis of conventional predictive DPC strategies and the improved approach are

presented in Section IV. Finally, concluding remarks are drawn in Section VI.

III. CONVENTIONAL PREDICTIVE DPC BASED ON VOLTAGE VECTOR SELECTION

With respect to conventional predictive DPC strategies, three voltage vectors including two active vectors and one zero vector are applied within each control period T_s . Active voltage vectors are often selected based on sector information of the grid-voltage vector, as shown in Table I.

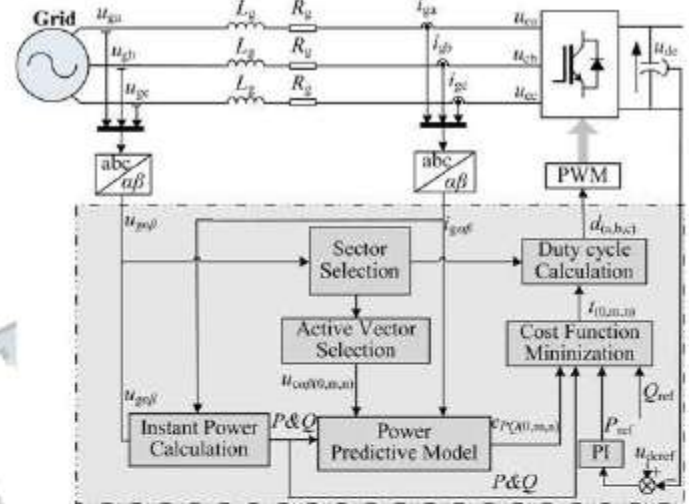


Fig. 1. Block diagram of the conventional predictive DPC strategy.

The errors of predicted active and reactive power at the end of k th control period can be computed as

$$EP = P_{gref} - P_g - 2eP_0 t_0 - 2eP_{mtm} - 2eP_{ntn} \quad (1)$$

$$EQ = Q_{gref} - Q_g - 2eQ_0 t_0 - 2eQ_{mtm} - 2eQ_{ntn} \quad (2)$$

where eP_m and eP_n denote active power variation rates caused by the active voltage vectors V_m and V_n within one sample period T_s . eQ_m and eQ_n are reactive power variation rates caused by V_m and V_n within T_s . eP_0 and eQ_0 denote active and reactive power variation rates caused by zero voltage vectors, respectively. t_m and t_n are t/e application time of V_m and V_n within $T_s/2$, respectively. t_0 represents the application time of zero vectors within $T_s/2$. t_m , t_n , and t_0 satisfy the boundary condition $t_0 + t_m + t_n = T_s/2$.

For conventional predictive DPC strategies, least-square optimization method is often adopted. The cost function is constructed as

$$W = EP^2 + EQ^2. \quad (3)$$

Once t_m and t_n are predicted by minimizing W , switch duty cycles can thus be obtained and switch signals are generated, as demonstrated in Table II, where d_a , d_b , and d_c denote three phase duty cycles, respectively. Fig. 1 shows

the block diagram of the conventional predictive DPC strategy. The corresponding flowchart of the control strategy is given in Fig.2. Figs. 1 and 2 indicate that the sector information and active voltage vector selection are both essential for conventional predictive DPCs. Selection of two active voltage vectors is based on the sector information. Besides, when duty cycles are to be computed, sector information is also required, as demonstrated in Fig. 2.

IV. ANALYSIS OF CONVENTIONAL PREDICTIVE DPC STRATEGY AND THE IMPROVED APPROACH

Taking Sector V for example, when the grid-voltage vector is located in Sector V, V_5 and V_6 are normally selected as active vectors.

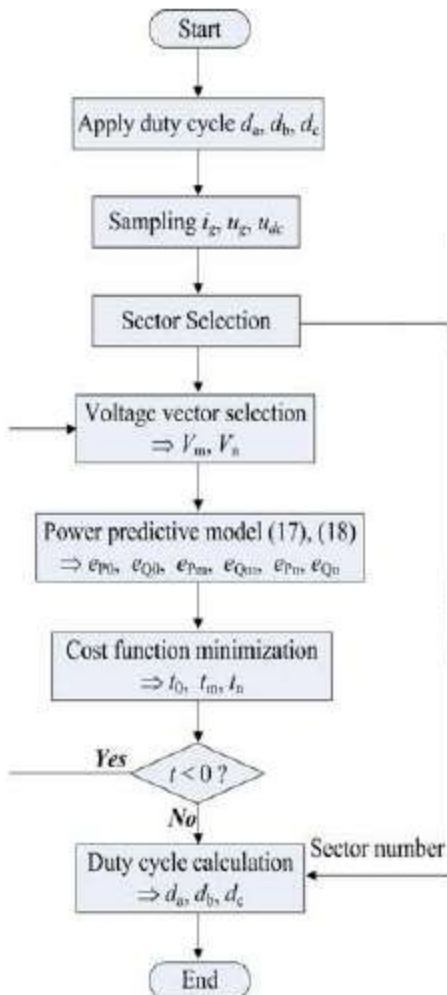


Fig. 2. Flowchart of the conventional predictive DPC strategy.

Their application time t_5 and t_6 will be calculated by minimizing W , the sum of squared power errors.

Obviously, the length of active vectors can be denoted as $V_5 \cdot t_5$ and $V_6 \cdot t_6$, respectively. For clear illustrations, decomposition and reconstruction of voltage vectors in the vector space are depicted in Fig. 3.

Vector $V_6 \cdot t_6$ can be synthesized using a combination of the two adjacent vectors

$$V_6 \cdot t_6 = V_1 \cdot t_6 + V_5 \cdot t_6 \tag{4}$$

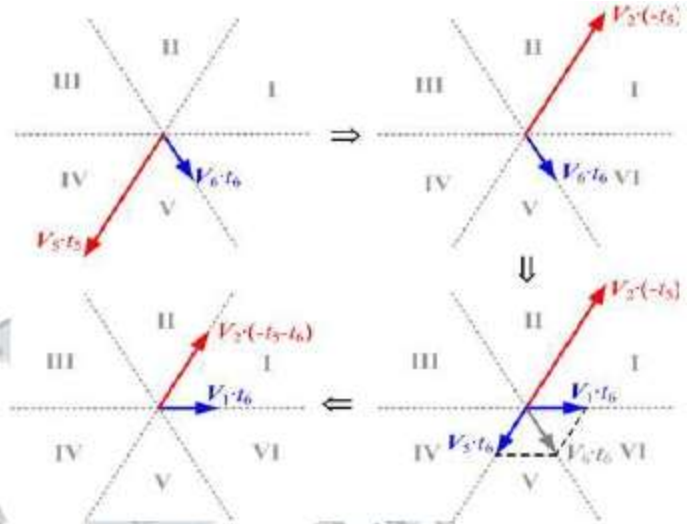


Fig.3. Decomposition and reconstruction of $V_5 \cdot t_5 + V_6 \cdot t_6$ in the vector space.

Therefore, the following equations can be obtained

$$\begin{aligned} V_5 \cdot t_5 + V_6 \cdot t_6 &= V_5 \cdot t_5 + V_1 \cdot t_6 + V_5 \cdot t_6 \\ &= V_5 \cdot (t_5 + t_6) + V_1 \cdot t_6 \end{aligned} \tag{5}$$

According to the equivalence principle, the following rules are obeyed:

$$V_5 \cdot (t_5 + t_6) = -[V_2 \cdot (t_5 + t_6)] = V_2 \cdot (-t_5 - t_6) \tag{6}$$

Substituting (21) into (20), yields

$$V_5 \cdot t_5 + V_6 \cdot t_6 = V_1 \cdot t_6 + V_2 \cdot (-t_5 - t_6) \tag{7}$$

It is clearly visible in (23) that the effects of $V_5 \cdot t_5$ along with $V_6 \cdot t_6$ equals to the synthesis of $V_1 \cdot t_6$ and $V_2 \cdot (-t_5 - t_6)$. When the conventional predictive DPC strategy is adopted, V_5 and V_6 are normally selected as active vectors when the grid-voltage vector is located in Sector V. The optimal set of application time t_5 and t_6 can thus be obtained. However, it is implied by (23) that, if V_1 and V_2 are selected when the grid-voltage vector is located in Sector V, their optimal application time can also be calculated out similarly. This will surely result in minimization of W . This indicates that, when the grid-voltage vector is located in Section V, V_1 and V_2 can also be selected, instead of V_5 and V_6 , which will not affect the minimization of power errors. Similarly, when the grid-

voltage vector is located in other sections, V_1 and V_2 can always be selected, and their application time can be calculated and implemented.

This is a remarkable conclusion, which builds a solid base for the proposed predictive control strategy without sector information and voltage vector selection. For the purpose of convenience, t_1' and t_2' are denoted as application time for V_1 and V_2 , respectively. Different combinations of voltage vectors can thus be expressed by $V_1, V_2, t_1',$ and t_2' as follows:

$$\begin{aligned} V_1 \cdot t_1' + V_2 \cdot t_2' &= V_2 \cdot (t_1' + t_2') + V_3 \cdot (-t_1') \\ &= V_3 \cdot t_2' + V_4 \cdot (-t_1' - t_2') \\ &= V_4 \cdot (-t_1') + V_5 \cdot (-t_2') \\ &= V_5 \cdot (-t_1' - t_2') + V_6 \cdot t_1' \\ &= V_6 \cdot (-t_2') + V_1 \cdot (t_1' + t_2'). \end{aligned} \quad (8)$$

It is implied that within all six sectors, different combinations of voltage vectors can always be equivalently replaced by V_1 and V_2 , with completely different application time.

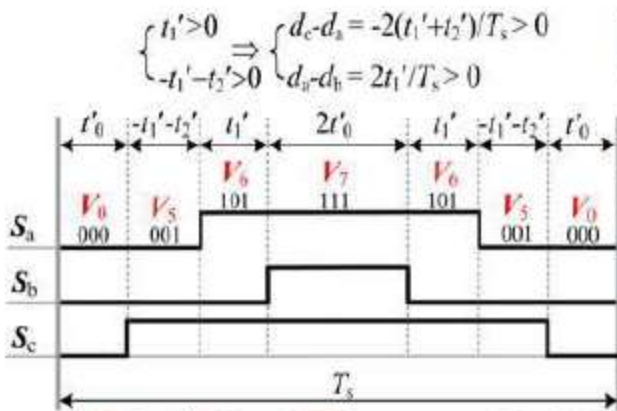


Fig.4. Switch signals in case of $-t_1' - t_2' > 0$ and $t_1' > 0$.

TABLE II
ACTUAL ACTIVE VECTORS AND THE CORRESPONDING RELATIONSHIP

Time relationship	Actual active vectors	Duty cycle relationship
$t_1' > 0, t_2' > 0$	V_1, V_2	$d_c > d_b > d_a$
$t_1' + t_2' > 0 \ \& \ -t_1' > 0$	V_2, V_3	$d_b > d_a > d_c$
$t_2' > 0 \ \& \ -t_1' - t_2' > 0$	V_3, V_4	$d_c > d_b > d_a$
$-t_1' > 0 \ \& \ -t_2' > 0$	V_4, V_5	$d_c > d_b > d_a$
$-t_1' - t_2' > 0 \ \& \ t_1' > 0$	V_5, V_6	$d_c > d_a > d_b$
$-t_2' > 0 \ \& \ t_1' + t_2' > 0$	V_6, V_1	$d_a > d_c > d_b$

This, as a result, indicates that, no matter where the grid-voltage vector is located, V_1 and V_2 can always be

selected. Their optimal application time, t_1' and t_2' , can thus be calculated out based on cost function minimization. According to the first line of Table.3.4.1.a, switch duty cycles can be directly obtained based on t_1' and t_2'

$$\text{---} \quad (9)$$

$$\text{---} \quad (10)$$

$$\text{---} \quad (11)$$

However, it should be noted that, even though V_1 and V_2 are always selected and duty cycles are calculated based on the first line of Table.I, V_1 and V_2 are not the actual active voltage vectors in most cases. Taking Sector V for example, when the grid-voltage vector is located in most part of this sector, V_5 and V_6 should be the actual active vectors. Their application time should be larger than zero. According to (24), if V_1 and V_2 are selected under this situation, the calculated application time t_1' and t_2' satisfy $t_1' > 0$ and $-t_1' - t_2' > 0$. For clear illustration, switch signals in this case are depicted in Fig. 4

It is demonstrated in Fig. 4 that, even though V_1 and V_2 are always selected and duty cycles are calculated based on the first line of Table II, the actual voltage vector implemented remains V_5 (001) and V_6 (101), as long as t_1' and t_2' satisfy $t_1' > 0$ and $-t_1' - t_2' > 0$. Similarly, based on (3.5), the actual active vectors and the corresponding numerical relationship among the calculated application time can be obtained, as shown in Table.II

Obviously, switch duty cycles should be larger than zero, and be smaller than one. However, switch duty cycles calculated based on (25), (26), and (27), might exceed this scope. This phenomenon should be taken into account in real control systems. As shown in Fig.4, the application time $-2(t_1' + t_2')$ for V_5 is directly proportional to $d_c - d_a$. Similarly, the application time $2t_1'$ for V_6 is proportional to $d_a - d_b$. Detailed relationship between duty cycles and duration time of actual active vectors are shown in Table.III.

As clearly visible in Table III, as long as $d_a - d_b$ and $d_b - d_c$ remain unchanged, the application time of actual active vectors will be the same. This indicates that, if the calculated duty cycle exceeds the conventional scope, i.e., $d < 0$ or $d > 1$, they can be equivalently reconstructed, as long as $d_a - d_b$ and $d_b - d_c$ remain unchanged. Besides, for the purpose of suppressing power fluctuations, application time of zero vectors is symmetrically distributed within one sampling period. The effectiveness of symmetrical distribution will be further confirmed by experimental results in the following sections.

Based on the analysis previously mentioned, reconstruction of duty cycles can thus be outlined as follows. $d_a, d_b,$ and d_c are first arranged in order from largest to smallest in value, $d_{max}, d,$ and d_{min} . For example,

$$d_{\max} = d_b, \quad d_{\min} = d_a, \quad d = d_c .$$

(12)

The differences $d_{\max} - d$ and $d - d_{\min}$ can thus be obtained, which are proportional to the application time of active voltage vectors. Consequently, $d_0 = 1 - (d_{\max} - d) - (d - d_{\min}) = 1 - (d_{\max} - d_{\min})$ is proportional to the application time for zero vectors. For the purpose of symmetrically distributed and taking into consideration, the new duty cycles d_a' , d_b' , and d_c' can be further represented as

$$d'_a = d'_c - (d_c - d_a) = 1 - d_0 - d_b + d_a \quad (13)$$

$$d'_b = 1 - d_0$$

(14)

$$d'_c = d'_b - (d_b - d_c) = 1 - d_0 - d_b + d_c .$$

(15)

For better understanding, reconstruction of duty cycles when the value d_b calculated out exceeds the scope ($d_b > 1$). Besides, power variations when voltage vectors are symmetrically and unsymmetrically distributed respectively. It is clearly visible in these two figures that, when the voltage vectors are symmetrically distributed, power variations are much smaller than those obtained with unsymmetrical distribution of voltage vectors. This aspect will be further validated by experimental results in the following sections.

Furthermore, the control region of voltage vectors is an important aspect for power converter controllers. If the control vector is outside the control region of power converters, i.e., $d_{\max} - d_{\min} > 1$, the new duty cycles d_a' , d_b' , and d_c' should be calculated by

(16)

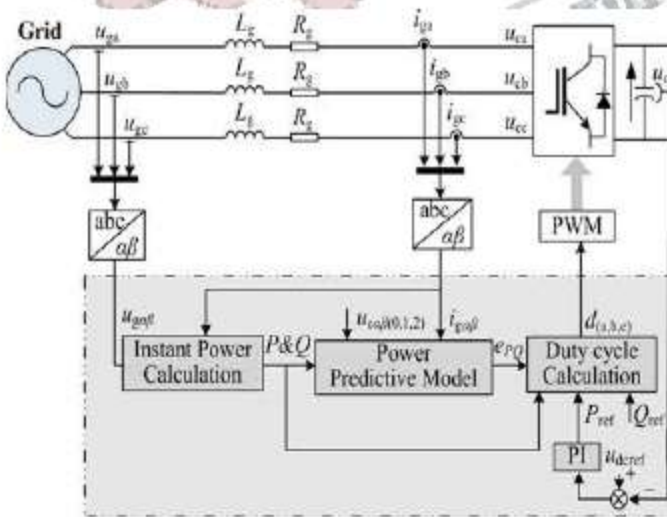


Fig.5. Block diagram of the proposed predictive DPC strategy.

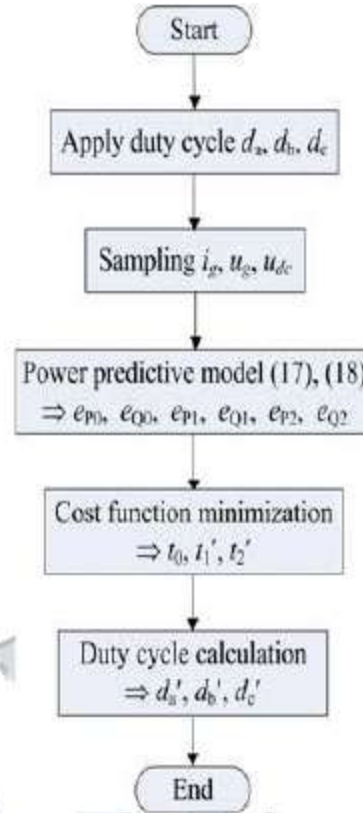


Fig. 6. Flowchart of the proposed predictive DPC strategy.

For better understanding, reconstruction of duty cycles when the control vector lies outside the control region ($d_{\max} - d_{\min} > 1$). Overall, the execution process and the block diagram of the proposed predictive control strategy can be outlined and its flowchart is shown in Fig.6.

Sector information is not required here, and selection of active voltage vectors is also eliminated. Therefore, incorrect selection of voltage vectors and the resulting performance deterioration will surely be avoided, without the need of any additional compensation measures.

V. FUZZY LOGIC CONTROLLER

Fuzzy logic idea is similar to the human being's feeling and inference process. Unlike classical control strategy, which is a point-to-point control, fuzzy logic control is a range-to-point or range-to-range control. The output of a fuzzy controller is derived from fuzzification of both inputs and outputs using the associated membership functions. A crisp input will be converted to the different members of the associated membership functions based on its value. From this point of view, the output of a fuzzy logic controller is based on its memberships of the different membership functions, which can be considered as a range of inputs.

Fuzzy ideas and fuzzy logic are so often utilized in our routine life that nobody even pays attention to them.

For instance, to answer some questions in certain surveys, most time one could answer with 'Not Very Satisfied' or 'Quite Satisfied', which are also fuzzy or ambiguous answers.

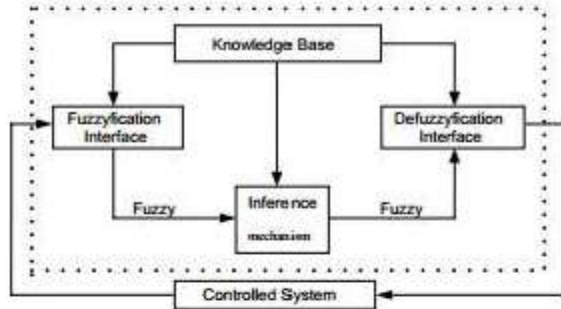


Fig. 7. Fuzzy Logic Controller.

Exactly to what degree is one satisfied or dissatisfied with some service or product for those surveys? These vague answers can only be created and implemented by human beings, but not machines. Is it possible for a computer to answer those survey questions directly as a human beings did? It is absolutely impossible. Computers can only understand either '0' or '1', and 'HIGH' or 'LOW'. Those data are called crisp or classic data and can be processed by all machines. Is it possible to allow computers to handle those ambiguous data with the help of a human being? If so, how can computers and machines handle those vague data? The answer to the first question is yes. But to answer the second question, we need some fuzzy logic techniques and knowledge of fuzzy inference system.

The basic configuration of the FLC can be simply represented in four parts, as shown in figure.

1. Fuzzification module – the functions of which are first, to read, measure, and scale the control variable (speed, acceleration) and, second, to transform the measured numerical values to the corresponding linguistic (fuzzy variables with appropriate membership values);
2. Knowledge base - this includes the definitions of the fuzzy membership functions defined for each control variables and the necessary rules that specify the control goals using linguistic variables;
3. Inference mechanism – it should be capable of simulating human decision making and influencing the control actions based on fuzzy logic;
4. Defuzzification module – which converts the inferred decision from the linguistic variables back the numerical values.

Fuzzy logic techniques have been widely applied in all aspects in today's society. To implement fuzzy logic technique to a real application requires the following three steps:

1. Fuzzification – convert classical data or crisp data into fuzzy data or Membership Functions (MFs)
2. Fuzzy Inference Process – combine membership functions with the control rules to derive the fuzzy output
3. Defuzzification – use different methods to calculate each associated output and put them into a table: the lookup table. Pick up the output from the lookup table based on the current input during an application As mentioned before, all machines can process crisp or classical data such as either '0' or '1'.

In order to enable machines to handle vague language input such as 'Somehow Satisfied', the crisp input and output must be converted to linguistic variables with fuzzy components. For instance, to control an air conditioner system, the input temperature and the output control variables must be converted to the associated linguistic variables such as 'HIGH', 'MEDIUM', 'LOW' and 'FAST', 'MEDIUM' or 'SLOW'. The former is corresponding to the input temperature and the latter is associated with the rotation speed of the operating motor. Besides those conversions, both the input and the output must also be converted from crisp data to fuzzy data. All of these jobs are performed by the first step – fuzzification. In the second step, to begin the fuzzy inference process, one need combine the Membership Functions with the control rules to derive the control output, and arrange those outputs into a table called the lookup table.

VI. PULSE WIDTH MODULATION

The most efficient method of controlling output voltage is to incorporate PWM control within inverters. In this method, a fixed dc voltage is supplied to inverter and a controlled ac output voltage is obtained by adjusting on-off period of inverter devices. Pulse Width Modulation variable speed drives are increasingly applied in many new industrial applications that require superior performance. Recently, developments in power electronics and semiconductor technology have lead improvements in power electronic systems. Hence, different circuit configurations namely PWM inverters have become popular and considerable interest by researcher are given on them.

A number of Pulse width modulation (PWM) schemes are used to obtain variable voltage and frequency supply. The most widely used PWM scheme for voltage source inverters is sinusoidal PWM. Because of advances in solid state power devices and microprocessors, switching power converters are used in industrial application to convert and deliver their required energy to the motor or load. PWM signals are pulse trains with fixed frequency and magnitude and variable pulse width. There is one pulse of fixed magnitude in every PWM period. However, the width of the pulses changes from pulse to pulse according to a modulating signal.

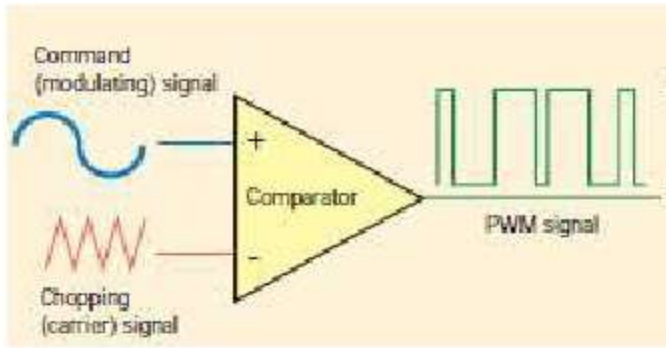


Fig.8.Pulse Width Modulation

When a PWM signal is applied to the gate of a power transistor, it causes the turn on and turns off intervals of the transistor to change from one PWM period to another PWM period according to the same modulating signal. The frequency of a PWM signal must be much higher than that of the modulating signal, the fundamental frequency, such that the energy delivered to the motor and its load depends mostly on the modulating signal. The AC/DC converters consist of power electronics devices like Insulated Gate Bipolar Transistors (IGBT) or Gate Turn-Off thyristors (GTO) that are characterized by switch mode operation. The capability of forming sinusoidal currents is provided by the introduction of the sophisticated technique called Pulse-Width Modulation (PWM). This technique provides the sequences of width-modulated pulses to control power switches. Many PWM techniques have been developed according to special requirements and optimization criteria. The choice of the particular PWM technique arises from the de-sired performance of the synchronous rectifiers.

A PWM signal consists of two main components that define its behavior: a duty cycle and a frequency. The duty cycle describes the amount of time the signal is in a high (on) state as a percentage of the total time of it takes to complete one cycle. The frequency determines how fast the PWM completes a cycle (i.e. 1000 Hz would be 1000 cycles per second), and therefore how fast it switches between high and low states. By cycling a digital signal off and on at a fast enough rate, and with a certain duty cycle, the output will appear to behave like a constant voltage analog signal when providing power to devices.

Duty cycle is a proportion of time during which a device is operated. Reference value of active and reactive power is given as input. Using the formula, duty cycle is calculated.

$$\text{Duty cycle} = \frac{T_{on}}{\text{Time Period}}$$

$$\text{Time period} = T_{on} + T_{off}$$

T_{on} - on time,
 T_{off} - off time

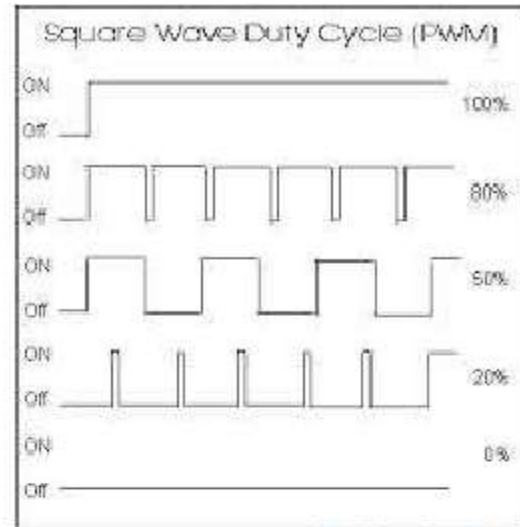


Fig.9. Square Wave Duty Cycle

VII. SIMULATION DIAGRAM AND WAVEFORMS

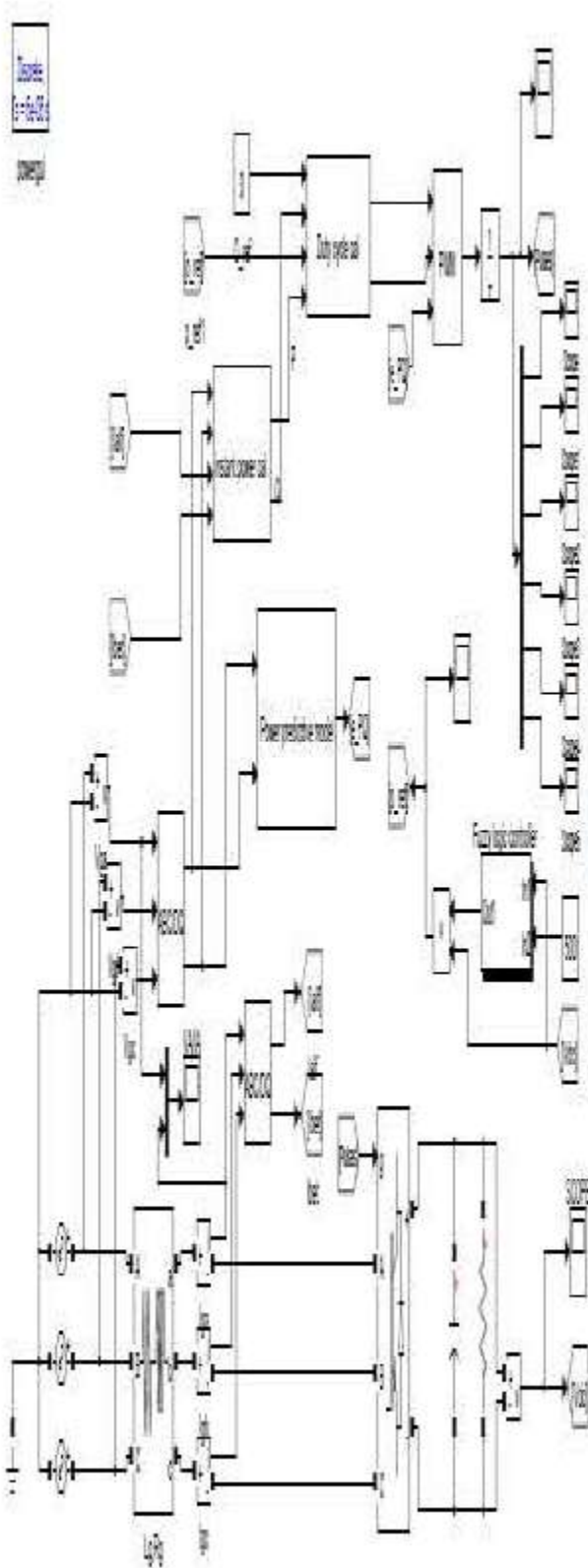


Fig.10. Simulation Diagram of P-DPC.

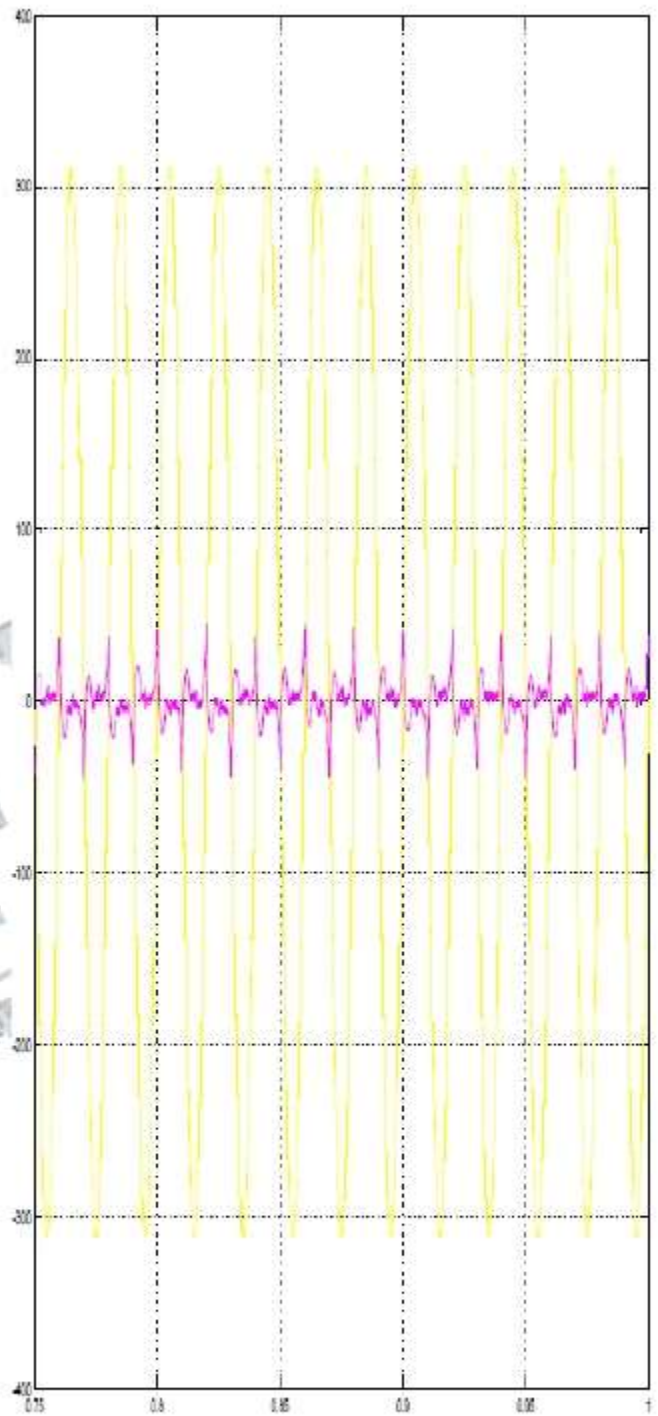


Fig.11.Input waveform(Va/Ia)

X axis: Time in seconds.

Y axis: Voltage in volts and Current in amps.

Voltage Value: 311V AC,

Current value:35 A.

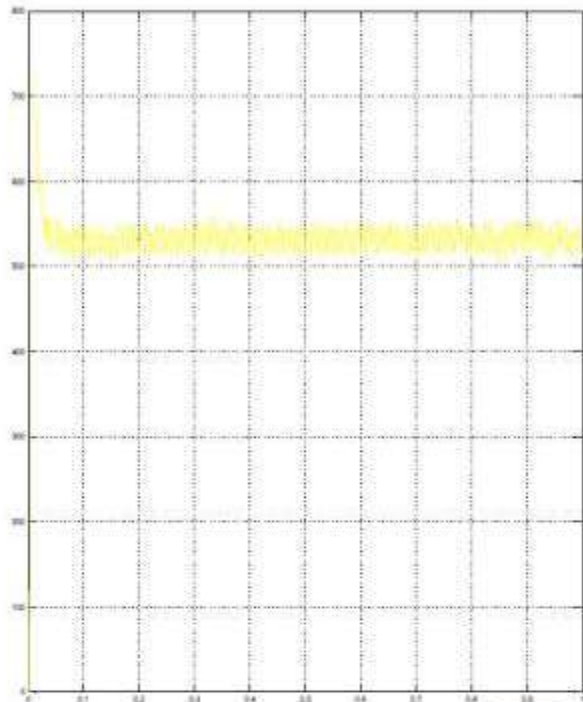


Fig. 12. Output Voltage Waveform for Reference Value 500

X axis: Time in seconds.
Y axis: Voltage in volts.
Output Voltage: 500V.

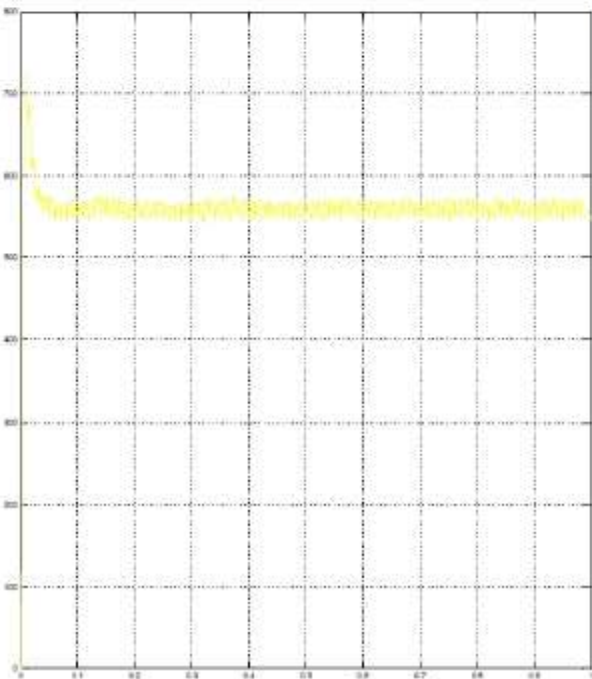


Fig.13. Output Voltage for Reference Value 550.

X axis: Time in seconds.

Y axis: Voltage in volts. Output Voltage: 550V.

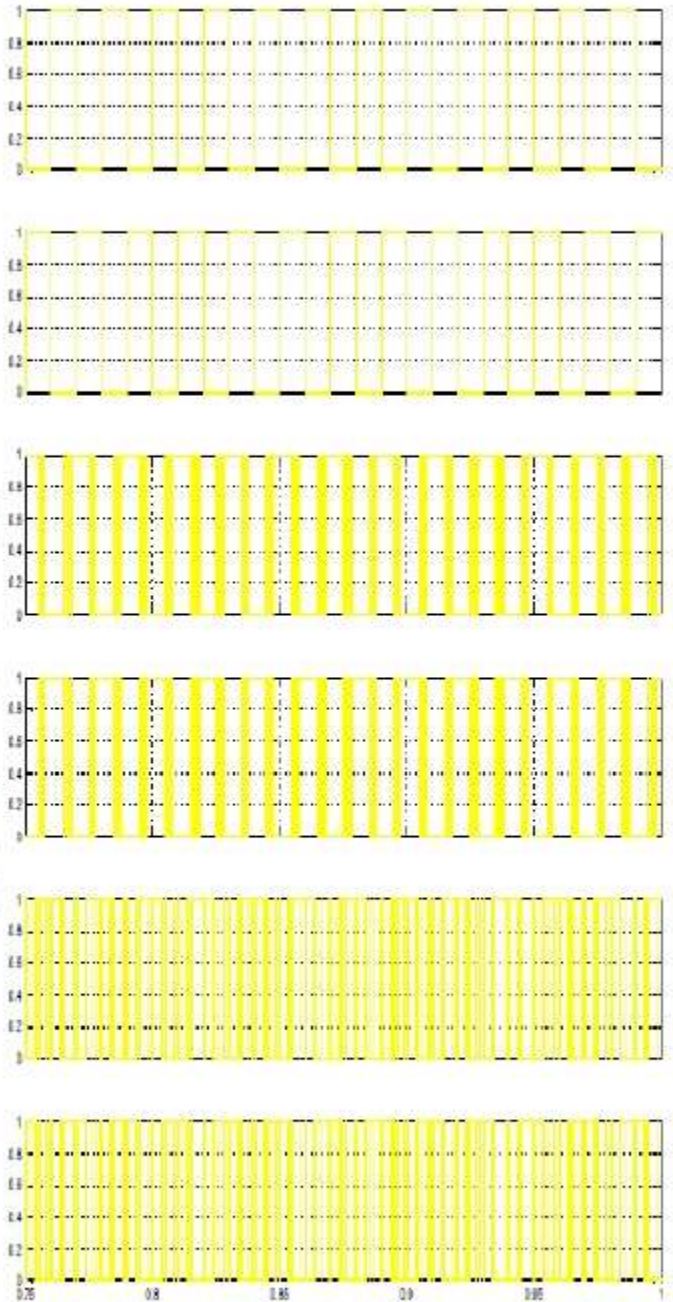


Fig.14 . Duty Cycle for Switches 1-6.

X axis: Time in seconds.

Y axis: Amplitude in volts.

VIII. CONCLUSION

Normally, when predictive DPC strategies are implemented, two active voltage vectors are first selected according to the angular information of the grid-voltage vector. Different from conventional predictive power control strategies, an improved predictive DPC method is proposed in this paper. Fixed voltage vectors are always adopted, instead of selecting voltage vectors according to the angular information of the grid-voltage vector or the virtual-flux vector. The converter switching time is obtained by minimizing the squared errors of the instantaneous active and reactive power. Switch duty cycles are then calculated and equivalently reconstructed for symmetrical distribution of voltage vectors. Experimental results show that the proposed strategy not only presents rapid dynamic response due to the use of the predictive controller, but also possesses excellent steady-state performance as a result of duty cycle reconstruction. Besides, sector information is not required here, and selection of active voltage vectors is also eliminated. Therefore, incorrect selection of voltage vectors and the resulting performance deterioration are surely avoided, without the need of any additional compensation measures.

IX REFERENCE

- [1] J. R. Rodriguez, J. W. Dixon, J. R. Espinoza, J. Pontt, and P. Lezana, "PWM regenerative rectifiers: State of the art," *IEEE Trans. Ind. Electron.*, vol. 52, no. 1, pp. 5–22, Feb. 2005.
- [2] K. J. Lee, B. G. Park, R. Y. Kim, and D. S. Hyun, "Robust predictive current controller based on a disturbance estimator in a three-phase grid connected inverter," *IEEE Trans. Power Electron.*, vol. 27, no. 1, pp. 276–283, Jan. 2012.
- [3] E. C. Santos, C. B. Jacobina, E. R. Silva, and N. Rocha, "Single-phase to three-phase power converters: State of the art," *IEEE Trans. Ind. Electron.*, vol. 27, no. 5, pp. 2437–2452, May 2012.
- [4] Z. Song, C. Xia, and T. Liu, "Predictive current control of three-phase grid connected converters with constant switching frequency for wind energy systems," *IEEE Trans. Ind. Electron.*, vol. 60, no. 6, pp. 2451–2464, Jun. 2013.
- [5] Y. Zhang, W. Xie, Z. Li, and Y. Zhang, "Model predictive direct power control of a PWM rectifier with duty cycle optimization," *IEEE Trans. Power Electron.*, vol. 28, no. 11, pp. 5343–5351, Nov. 2013.
- [6] J. A. Restrepo, J. M. Aller, A. Bueno, J. C. Viola, A. Berzoy, R. Harley, and T. G. Habetler, "Direct power control of a dual converter operating as a synchronous rectifier," *IEEE Trans. Power Electron.*, vol. 26, no. 5, pp. 1410–1417, May 2011.
- [7] J. G. Norniella, J. M. Cano, G. A. Orcajo, C. Garcia, J. F. Pedrayes, M. F. Cabanas, and M. G. Melero, "Analytic and iterative algorithms for online estimation of coupling inductance in direct power control of three phase active rectifiers," *IEEE Trans. Power Electron.*, vol. 26, no. 11, pp. 3298–3307, Nov. 2011.
- [8] H. Nian and Y. Song, "Direct power control of doubly fed induction generator under distorted grid voltage," *IEEE Trans. Power Electron.*, vol. 29, no. 2, pp. 894–905, Feb. 2014.
- [9] J. G. Norniella, J. M. Cano, G. A. Orcajo, C. H. R. Garcia, J. F. Pedrayes, M. E. Cavbanas, and M. G. Melero, "Analytic and iterative algorithms for online estimation of coupling inductance in direct power control of three phase active rectifiers," *IEEE Trans. Power Electron.*, vol. 26, no. 11, pp. 3298–3307, Nov. 2011.
- [10] J. A. Mart'inez, J. E. Carrasco, and S. Arnaltes, "Table-based direct power control: A critical review for microgrid applications," *IEEE Trans. Power Electron.*, vol. 25, no. 12, pp. 2949–2961, Dec. 2010.
- [11] A. Sato and T. Noguchi, "Voltage-source PWM rectifier-inverter based on direct power control and its operation characteristics," *IEEE Trans. Power Electron.*, vol. 26, no. 5, pp. 1559–1567, May 2011.
- [12] A. Bouafia, F. Krim, and J. P. Gaubert, "Fuzzy-logic-based switching stage selection for direct power control of three-phase PWM rectifier," *IEEE Trans. Ind. Electron.*, vol. 56, no. 6, pp. 1984–1992, Jun. 2009.
- [13] T. Noguchi, H. Tomiki, S. Kondo, and I. Takahashi, "Direct power control of PWM converter without power-source voltage sensors," *IEEE Trans. Ind. Appl.*, vol. 34, no. 3, pp. 473–479, May/Jun. 1998.
- [14] M. Malinowski, M. P. Kazmierkowski, S. Hansen, F. Blaabjerg, and G. D. Marques, "Virtual-flux-based direct power control of three-phase PWM rectifiers," *IEEE Trans. Ind. Appl.*, vol. 37, no. 4, pp. 1019–1027, Jul./Aug. 2001.
- [15] Y. Zhang, Z. Li, Y. Zhang, W. Xie, Z. Piao, and C. Hu, "Performance improvement of direct power control of PWM rectifier with simple calculation," *IEEE Trans. Power Electron.*, vol. 28, no. 7, pp. 3428–3437, Jul. 2013.
- [16] D. Zhi, L. Xu, and B. W. Williams, "Improved direct power control of grid-connected DC/AC converters," *IEEE Trans. Power Electron.*, vol. 24, no. 5, pp. 1280–1292, May 2009.
- [17] J. A. Restrepo, J. M. Aller, J. C. Viola, A. Bueno, and T. G. Habetler, "Optimum space vector computation technique for direct power control," *IEEE Trans. Power Electron.*, vol. 24, no. 6, pp. 1637–1645, Jun. 2009.
- [18] M. Malinowski, M. Jasiński, and M. P. Kazmierkowski, "Simple direct power control of three-phase PWM rectifier using space-vector modulation (DPC-SVM)," *IEEE Trans. Ind. Electron.*, vol. 51, no. 2, pp. 447–454, Apr. 2004.
- [19] S. Vazquez, J. A. Sanchez, J. M. Carrasco, J. I. Leon, and E. Galvan, "A model-based direct power control for

- three-phase power converters,” *IEEE Trans. Ind. Electron.*, vol. 55, no. 4, pp. 1647–1657, Apr. 2008.
- [20] R. Portillo, S. Vazquez, J. I. Leon, M. M. Prats, and L. G. Franquelo, “Model based adaptive direct power control for three-level NPC converters,” *IEEE Trans. Ind. Inform.*, vol. 9, no. 2, pp. 1148–1157, May 2013.
- [21] P. Cortés, M. P. Kazmierkowski, R. M. Kennel, D. E. Quevedo, and J. Rodríguez, “Predictive control in power electronics and drives,” *IEEE Trans. Ind. Electron.*, vol. 55, no. 12, pp. 4312–4324, Dec. 2008.
- [22] P. Cortés, J. Rodríguez, P. Antoniewicz, and M. P. Kazmierkowski, “Direct power control of an AFE using predictive control,” *IEEE Trans. Power Electron.*, vol. 23, no. 5, pp. 2516–2523, Sep. 2008.
- [23] J. Hu, J. Zhu, Y. Zhang, G. Platt, Q. Ma, and D. G. Dorrell, “Predictive direct virtual torque and power control of doubly fed induction generators for fast and smooth grid synchronization and flexible power regulation,” *IEEE Trans. Power Electron.*, vol. 28, no. 7, pp. 3182–3194, Jul. 2013.
- [24] S. S. Davari, D. Khaburi, and R. Kennel, “An improved FCS–MPC algorithm for an induction motor with an imposed optimized weighting factor,” *IEEE Trans. Power Electron.*, vol. 27, no. 3, pp. 1540–1551, Mar. 2012.
- [25] D. E. Quevedo, R. P. Aguilera, M. A. Perez, P. Cortes, and R. Lizana, “Model predictive control of an AFE rectifier with dynamic references,” *IEEE Trans. Power Electron.*, vol. 27, no. 7, pp. 3128–3136, Jul. 2012.

